Hydrogen-Bonded Complexes of Phenylacetylene with Water, Methanol, Ammonia, and Methylamine. The Origin of Methyl Group-Induced Hydrogen Bond Switching

Robert Sedlak,[†] Pavel Hobza,*,[†,‡] and G. Naresh Patwari*,[§]

Institute of Organic Chemistry and Biochemistry, Academy of Sciences of the Czech Republic and Center for Biomolecules and Complex Molecular Systems, Flemingovo nám. 2, 166 10 Prague 6, Czech Republic, Department of Physical Chemistry, Palacký University, 771 46 Olomouc, Czech Republic, and Department of Chemistry, Indian Institute of Technology Bombay, Powai, Mumbai 400076 India

The infrared spectra in the acetylenic C—H stretching region for the complexes of phenylacetylene with water, methanol, ammonia, and methylamine are indicative of change in the intermolecular structure upon substitution with a methyl group. High-level ab initio calculations at CCSD(T)/aug-cc-pVDZ level indicate that the observed complexes of water and ammonia are energetically the most favored structures, and electrostatics play a dominant role in stabilizing these structures. The ability of the π electron density of the benzene ring to offer a larger cross-section for the interaction and the increased polarizability of the O—H and N—H groups in methanol and methylamine favor the formation of π hydrogen-bonded complexes, in which dispersion is the dominant force. Further, the observed phenylacetylene—methylamine complex can be tentatively assigned to a kinetically trapped higher energy structure. The observed methyl group-induced hydrogen bond switching in the phenylacetylene complexes can be attributed to the switching of the dominant interaction from electrostatic to dispersion.

Introduction

Phenylacetylene is perhaps the simplest multifunctional molecule to investigate competitive hydrogen bonding. It has three hydrogen bonding sites in the form of the benzene ring and the acetylenic C≡C bond, which can act as π acceptors, and an activated acetylenic C—H group, which can act as a σ donor. Further, with the absence of any strongly acidic/basic functional groups, the hierarchy of hydrogen sites cannot be determined on the basis of Etter and Legon—Millen rules.[1,2] One of the major challenges that needs to addressed in hydrogen bonding is to know, a priori, how the individual functional groups in multifunctional molecules will behave when they are made to interact with suitable hydrogen bonding partners. In multifunctional molecules the exact hydrogen bonding pattern will be a result of competition between various possibilities. Toward the goal of comprehending the hydrogen bonding behavior of multifunctional molecules, Patwari and co-workers investigated hydrogen-bonded complexes of phenylacetylene with various solvent molecules such as water, methanol, ammonia, methylamine, and other alcohols and amines.[3–5] The hydrogen-bonded complexes of phenylacetylene form a wide variety of intermolecular structures, which stem out of a subtle balance of intermolecular forces of various possible intermolecular structures.[3–5] For instance, phenylacetylene forms a quasiplanar cyclic complex with water, incorporating O—H···π and C—H···O hydrogen bonds.[3,4] In this case one of the O—H groups of a water molecule interacts with the π electron density of the C≡C bond, while the C—H group of the benzene ring in the ortho position is hydrogen-bonded to the oxygen atom of the water molecule. The structure of the phenylacetylene—water complex thus is different from both the benzene—water and acetylene—water complexes,[6,7] even though phenylacetylene incorporates the features of both benzene and acetylene. On the other hand, the the phenylacetylene—methanol complex is characterized by the presence of single O—H···π hydrogen bond, wherein the O—H group of methanol interacts with the π electron density of the benzene ring, similar to the benzene—methanol complex.[4] Phenylacetylene forms a linear C—H···N "σ" hydrogen-bonded complex with ammonia,[5] which is similar to acetylene—ammonia complex,[8] while the phenylacetylene—methylamine complex is characterized by the presence of a N—H···π hydrogen bond. In this case the N—H group of methylamine interacts with the π electron density of the benzene ring.[5] Such differences in the intermolecular structures of hydrogen-bonded complexes with water, methanol, ammonia, and methylamine involving benzene derivatives have not been reported in the literature prior to these complexes of phenylacetylene. These results illustrate that, in the case of interaction with multifunctional molecules, even minimal changes in the interacting partner, such as substitution by a ubiquitous methyl group, can result in dramatic change in the intermolecular structure. The change in the intermolecular structure with the substitution of a methyl group can be perceived as methyl group-induced hydrogen bond switching. In this article we address the underlying factors that influence the hydrogen bond switching observed in the complexes of phenylacetylene.

Methodology

The geometry optimizations were carried out at MP2(FC)/aug-cc-pVDZ level of theory, and in each case frequency calculations followed to ascertain the nature of the minima obtained. Single point calculations at CCSD(T)/aug-cc-pVDZ level were carried out on the MP2 level optimized structures. The stabilization energies were corrected for zero point energy

---

* Authors to whom correspondence should be addressed. E-mail: pavel.hobza@uochb.cas.cz (P.H.); naresh@chem.iitb.ac.in (G.N.P.).
† Academy of Sciences of the Czech Republic and Center for Biomolecules and Complex Molecular Systems.
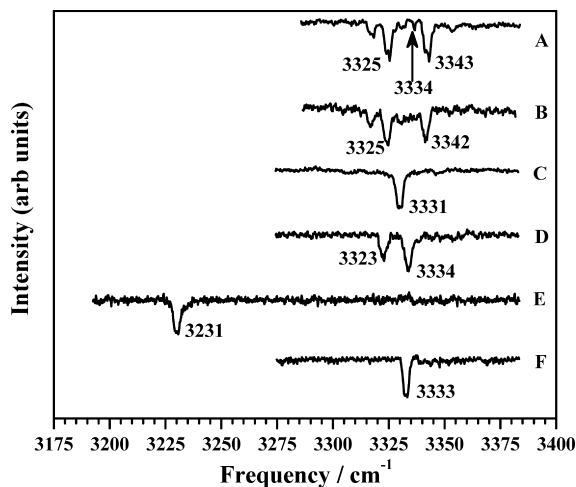‡ Palacký University.
§ Indian Institute of Technology Bombay.

Hydrogen-Bonded Complexes of Phenylacetylene

J. Phys. Chem. A, Vol. 113, No. 24, 2009 **6621**

Figure 1. The acetylenic C−H stretching region of the IR spectrum of (A) PHA, (B) PHA−Ar, (C) PHA−H_2O, (D) PHA−MeOH, (E) PHA−NH_3, and (F) PHA−$MeNH_2$. In A, the arrow indicates the position of the unperturbed C−H oscillator of PHA evaluated using the two-state deperturbation model (ref 13).

(ZPE) and basis set superposition error (BSSE). Thermochemical analysis, based on rigid rotor−harmonic oscillator−ideal gas approximations was also carried out using the vibrational frequency data obtained at MP2(FC)/aug-cc-pVDZ level of theory. Further, DFT-SAPT (symmetry adapted perturbation theory) calculations were performed with the aug-cc-pVDZ basis set.[9] This method allows for the separation of interaction energies into physically well-defined components, such as those arising from electrostatic, induction, dispersion, and exchange. The DFT-SAPT interaction energy (E^{int}) is given as

$$E^{int} = E_1^{Pol} + E_1^{Ex} + E_2^{Ind} + E_2^{Ex\text{-}Ind} + E_2^{D} + E_2^{Ex\text{-}D} + \delta HF \tag{1}$$

Equation 1 describes the electrostatic, exchange−repulsion, induction, exchange−induction, dispersion, and exchange−dispersion terms, while the last term is a Hartree−Fock correction for higher-order contributions to the interaction energy. In the present analysis the exchange−induction and exchange−dispersion terms will be included in the parent induction and dispersion terms. All calculations mentioned above were performed using the Gaussian03 and Molpro suite of programs.[10,11]

Results and Discussion

To begin with, the acetylenic C−H stretching region of the IR spectra of phenylacetylene and its complexes are reviewed to understand the structural assignment. The acetylenic C−H stretching regions of the infrared spectra for phenylacetylene (PHA) and its five complexes with argon (Ar), water (H_2O), methanol (MeOH), ammonia (NH_3), and methylamine ($MeNH_2$) are depicted in Figure 1. These spectra were recorded using the IR-UV double resonance spectroscopic method using either fluorescence or ion detection techniques.[3−5] The IR spectrum of PHA (trace A) shows the presence of two intense transitions at 3325 and 3343 cm^{-1}, which originate from Fermi resonance coupling between the acetylenic C−H stretching vibration and a combination band comprising one quantum of C≡C stretching and two quanta of C≡C−H out-of-plane bend.[12] A two-state deperturbation analysis places the unperturbed acetylenic C−H oscillator at 3334 cm^{-1} with the magnitude of coupling constant

to be 9 cm^{-1}.[13] In the case of PHA complexes any interaction that will perturb either the acetylenic C−H oscillator or the C≡C oscillator or both will lead to disappearance of Fermi resonance transitions. However, the perturbation should be about the order of the coupling constant of 9 cm^{-1} or more, in order completely remove the Fermi mixing. The Fermi resonance transitions of the PHA moiety, therefore, can be used a spectroscopic tool to probe the interactions present in various PHA complexes. Figure 1B depicts the IR spectrum of the PHA−argon complex, which is almost identical to that of bare PHA, within the experimental uncertainty of ±1 cm^{-1}.[13] This implies that the binding of Ar to PHA does not perturb either the C−H or the C≡C oscillators. It can therefore be inferred that the Ar atom is bound to the π electron density of the benzene ring in PHA.[13] This inference is substantiated by the structure of the PHA−Ar complex determined using the high-resolution REMPI spectrum for the $S_1 \leftarrow S_0$ electronic transition and microwave spectroscopy.[14]

The IR spectrum of PHA−H_2O complex, depicted in Figure 1C, consists of a single transition at 3331 cm^{-1}, which has been assigned to the acetylenic C−H stretching vibration. The acetylenic C−H stretching frequency shifts marginally (about 3 cm^{-1}) upon interaction with water, coupled with the loss of Fermi resonance coupling. This implies that the H_2O molecule interacts with the π electron density of the acetylenic C≡C bond.[3] Surprisingly, in the case of the PHA−MeOH (Figure 1D) complex, two transitions appear at 3323 and 3334 cm^{-1}, albeit with differences in the band positions and their intensities relative to bare PHA. These transitions have been assigned to the Fermi resonance bands.[4] The shift in the electronic transition for the $S_1\leftarrow 0$ relative to bare PHA, the shift in the O−H stretching frequency of the MeOH moiety, and the appearance of Fermi resonance transitions in the IR spectrum indicate that MeOH interacts with the π electron density of the benzene ring in PHA, resulting in formation of a O−H···π hydrogen-bonded complex.[4] The positions and the intensities of the Fermi resonance bands depend on the positions of the zero-order (unperturbed) oscillators and the coupling strength. The interaction of the methanolic O−H group with the π electron density of the benzene ring in PHA is expected to affect, marginally, both the zero-order positions and the coupling strength.

The assignment of the PHA−NH_3 complex to a C−H···N hydrogen-bonded complex is rather straightforward because the acetylenic C−H stretching vibration shifts by 103 cm^{-1} to a lower frequency (see Figure 1E). Surprisingly, the IR spectrum of PHA−$MeNH_2$, depicted in Figure 1F, shows a single transition at 3333 cm^{-1}. The acetylenic C−H stretching frequency shifts by −1 cm^{-1} upon interaction with $MeNH_2$, therefore completely ruling out the possibility of formation of a C−H···N hydrogen-bonded complex, similar to the PHA−NH_3 complex. It is well-known that the substitution of alkyl groups on NH_3 increases the basicity, which in-turn is expected to enhance the C−H···N hydrogen-bonded interaction. Such a consideration would indicate that the acetylenic C−H stretching frequency of PHA should be further lowered upon interaction with $MeNH_2$, relative to the NH_3 complex. The analysis of the IR spectrum along with the electronic spectrum leads to the assignment of a structure which is characterized by the formation of N−H···π (benzene π) hydrogen bonding along with a peripheral interaction between the methyl C−H group and the acetylenic C≡C bond.[5] One of the interesting observations about this complex is that the $MeNH_2$ behaves as a hydrogen bond donor, which is rather surprising considering that alkylamines are known to be excellent hydrogen bond acceptors and poor hydrogen bond donors. Additionally, examples in which the
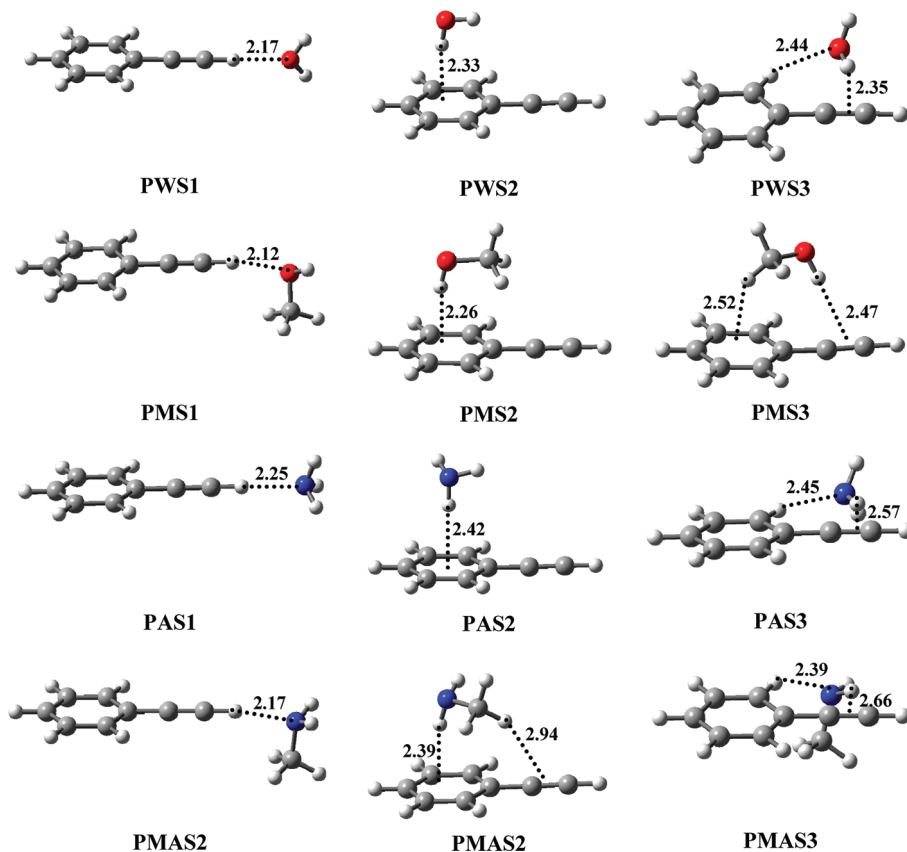
6622 *J. Phys. Chem. A, Vol. 113, No. 24, 2009*

Sedlak et al.

Figure 2. Calculated structures of PHA complexes with H_2O, MeOH, NH_3, and $MeNH_2$ at MP2/aug-cc-pVDZ level. The distances are shown in angstroms.

N—H group of aliphatic amines acts as a hydrogen bond donor are extremely sparse, to the extent of being nonexistent in the gas-phase complexes.[15]

The most interesting aspect, which has been observed for the PHA complexes, is the difference in the intermolecular structure between H_2O and MeOH complexes, and similarly between NH_3 and $MeNH_2$ complexes. These observations can be summed up as methyl group-induced hydrogen bond switching. To understand the origin of the observed hydrogen bond switching upon substitution with the methyl group, high-level ab initio calculations were carried out. First, geometries of the monomers and the complexes were optimized using MP2/aug-cc-pVDZ level of theory. Coincidentally, three minima were found for each set of complexes, structures of which are depicted in Figure 2. The first minimum in each case (**PWS1**, **PMS1**, **PAS1**, and **PMAS1**) is a linear C—H···O/N hydrogen-bonded complex, wherein the acetylenic C—H group acts as a hydrogen bond donor to the O/N atom of the acceptor, structures similar to acetylene—H_2O and acetylene—NH_3 complexes.[7,8] The second set of complexes are the π hydrogen-bonded complexes (**PWS2**, **PMS2**, **PAS2**, and **PMAS2**). In these cases the π electron density on the benzene ring of phenylacetylene is the hydrogen bond acceptor for the O—H/N—H groups of the interacting partner, similar to H_2O and NH_3 complexes of benzene.[6,16] In the third set, PHA forms a cyclic complexes with H_2O, NH_3, and $MeNH_2$, (**PWS3**, **PAS3**, and **PMAS3**). In these complexes, both PHA and the interacting molecule act as hydrogen bond donor and acceptor simultaneously, with the O—H/N—H group of the interacting molecule hydrogen-bonded to the π electron density of the C≡C of the acetylenic moiety in PHA. Further, the C—H group of the benzene ring in the ortho position is hydrogen-bonded to O/N of the accepting base. However, the

interaction of MeOH with the π electron density of the C≡C is distinctly different from the other three complexes. The MeOH complex, **PMS3**, can be characterized by the presence of O—H···π (acetylene π) and of C—H···π (benzene π) hydrogen bonds. Several attempts were made to obtain the cyclic structure starting from modified initial geometries; however, in all the cases, the calculations converged to the **PMS3** structure.

On the basis of the IR spectra in the acetylenic C—H stretching region (Figure 1) and other spectroscopic inputs,[17] the structures of H_2O, MeOH, NH_3, and $MeNH_2$ complexes were assigned to **PWS3**, **PMS2**, **PAS1**, and **PMAS2**, respectively.[3–5] These structural assignments were supplemented by stabilization energies calculated at MP2/aug-cc-pVDZ with ZPE and 50% BSSE correction.[3–5] The stabilization energies corrected for ZPE and 100% BSSE for all the complexes are listed in Table 1. However, with 100% BSSE correction, only the observed structures of PHA—MeOH (**PMS2**) and PHA—NH_3 (**PAS1**) were found to be global minima for the respective complexes, while the observed structures of PHA—H_2O (**PWS3**) and PHA—$MeNH_2$ (**PMAS2**) correspond to higher energy local minima (see Table 1). The MP2/aug-cc-pVDZ level is known to provide accurate geometries of isolated systems as well as molecular complexes.[18] On the other hand, it is also well-known that MP2 level calculations overestimate the dispersion energies and single point calculations at CCSD(T) level would provide a more accurate description.[19] Table 1 also lists ZPE and 100% BSSE corrected stabilization energies calculated at CCSD(T) level. The difference in the stabilization energies calculated at MP2 and CCSD(T) levels are only marginal for the C—H···O/N hydrogen-bonded complexes. However, the differences are substantial for rest of the complexes, which are characterized by the presence of π hydrogen bonding. This substantiates our

Hydrogen-Bonded Complexes of Phenylacetylene

J. Phys. Chem. A, Vol. 113, No. 24, 2009 **6623**

TABLE 1: ZPE and BSSE Corrected Stabilization Energies (kJ mol^{-1}) of Various PHA Complexes Calculated Using aug-cc-pVDZ Basis Set and ΔG for the Formation of Various Complexes at 10 K

	MP2	CCSD(T)	ΔG
PWS1	−6.4	−6.2	−5.6
PWS2	−8.1	−6.5	−6.3
PWS3	−7.6	−7.1	−7.0
PMS1	−9.8	−9.1	−8.6
PMS2	−13.6	−9.6	−8.3
PMS3	−13.1	−9.5	−8.7
PAS1	−8.7	−8.2	−8.3
PAS2	−5.4	−3.2	−2.8
PAS3	−6.7	−5.9	−5.6
PMAS1	−12.4	−11.3	−10.3
PMAS2	−10.6	−6.4	−5.6
PMAS3	−12.1	−9.4	−8.7

TABLE 2: DFT-SAPT Interaction Energy Decomposition (kJ mol^{-1}) for Various Complexes of PHA Calculated Using aug-cc-pVDZ Basis Set

	E_{elec}	E_{ind}	E_{disp}	E_{exch}	δ_{HF}	E_{int}	E_{int} + ZPE
PWS1	−17.0	−2.6	−6.4	17.4	−2.0	−10.6	−6.3
PWS2	−11.9	−2.7	−13.1	18.2	−1.5	−11.0	−7.3
PWS3	−25.5	−4.8	−13.6	32.2	−3.5	−15.2	−9.0
PMS1	−20.9	−3.1	−10.2	24.8	−2.8	−12.2	−9.0
PMS2	−17.4	−3.2	−26.1	36.2	−3.0	−13.5	−10.2
PMS3	−20.2	−3.2	−25.6	37.7	−3.2	−14.6	−10.7
PAS1	−24.9	−4.1	−8.4	27.0	−3.8	−14.2	−8.8
PAS2	−9.3	−1.4	−14.4	19.1	−1.4	−7.4	−3.9
PAS3	−22.4	−3.5	−13.8	29.8	−2.9	−12.8	−7.8
PMAS1	−29.2	−4.7	−12.7	35.9	−5.2	−16.0	−11.8
PMAS2	−15.4	−1.5	−26.3	35.2	−2.6	−10.6	−7.1
PMAS3	−25.5	−3.3	−23.1	41.1	−3.6	−14.4	−10.8

earlier statement that MP2 level calculations overestimate the dispersion energies. At CCSD(T) level the experimentally observed structure is the global minimum for the H$_2$O (**PWS3**), MeOH (**PMS2**), and NH$_3$ (**PAS1**) complexes. The PHA−MeNH$_2$ complex (**PMAS2**), however, is an exception and once again happens to be a higher energy local minimum.

The difference in stabilization energies for the three isomers of H$_2$O complexes is about 0.9 kJ mol^{-1}, while in the case of MeOH complexes this difference is only about 0.5 kJ mol^{-1}. However, in the case of NH$_3$ complexes the difference in the stabilization energy between the global minimum and the next higher energy local minimum is 2.3 kJ mol^{-1}. On the other hand, the observed PHA−MeNH$_2$ complex (**PMAS2**) is about 4.9 kJ mol^{-1} higher in energy than the global minimum. It must be pointed out here that even though the calculated energy differences between the various isomers are only marginal in the case of H$_2$O and MeOH complexes, while in the case of NH$_3$ and MeNH$_2$ complexes the differences are considerable, only one complex was observed experimentally in each case.[3−5]

The DFT-SAPT interaction energy decomposition was carried out for the all the structures shown in Figure 2. Table 2 lists the various components of the total energy and also the ZPE corrected SAPT stabilization energies. The ZPE corrected DFT-SAPT stabilization energies are comparable to the ZPE and BSSE corrected CCSD(T) energies using the same basis set (see Table 1). However, since the energy differences between the various minima are small, the change in the level of calculation leads to rearrangement of relative energies of various isomers in each set. In the case of DFT-SATP calculations, the observed complexes of H$_2$O and NH$_3$ are the global minima, while the complexes of MeOH and MeNH$_2$ are higher energy local minima. For the PHA−H$_2$O system, the observed complex

PWS3 has the highest contribution in all the columns, which implies that this structure maximizes all the possible interactions. In the case of MeOH complexes, the induction contribution is almost constant for all the three isomers. The formation of the observed **PMS2** structure is favored by the dispersion contribution, while the electrostatic contribution is the lowest among the three isomers. In the case of NH$_3$ complexes, higher contributions from electrostatic and induction energies play a dominant role in stabilizing the observed **PAS1** structure. On the other hand, the dispersion energy has a higher contribution in stabilizing the observed MeNH$_2$ complex, **PMAS2**. A careful inspection of Table 2 reveals that electrostatics plays major role in stabilizing the observed structures of H$_2$O and NH$_3$ complexes, while dispersion plays a major role in stabilizing the observed structures of MeOH and MeNH$_2$. This implies that the substitution by a methyl group switches the lead contribution from electrostatics to dispersion. This, in all probability, can be attributed to the higher polarizability of the O−H and N−H groups in MeOH and MeNH$_2$, respectively, which can be ascribed to the electron-donating ability of the methyl group.

Yet another parameter that was considered was the Gibbs free energy (ΔG) because the temperature of the experiment is nonzero and therefore the contribution of entropy cannot be neglected. The free energy surface includes the entropy contribution. The ΔG values were obtained by the thermochemical analysis following vibrational frequency calculations in Gaussian03 at MP2/aug-cc-pVDZ level of theory and the electronic energy obtained at CCSD(T)/aug-cc-pVDZ level. The Gibbs free energy (ΔG) for the formation of all the complexes was calculated as a function of temperature (T), and the results are presented in Figure 3. Further, the ΔG values at 10 K are listed in Table 1. These plots reveal that very low temperatures (below ∼100 K) are required for the formation and stability of all the complexes. For the H$_2$O complexes, below 80 K the ΔG for the formation of PWS3 is more negative than the other two complexes, and at 10 K, the experimentally observed PWS3 structure is clearly the most stable complex. In the case of MeOH complexes, the ΔG for the formation of the observed PMS2 structure is lower than the other two complexes by 0.4 kJ mol^{-1}, which are isoenergetic. With the energy separation of 0.4 kJ mol^{-1}, the combined population of the other two species relative to **PMS2** at 10K will be less than 2%. For NH$_3$ complexes, the **PAS1** structure is clearly favored over the other two structures in the entire temperature range while, in the case of MeNH$_2$, the observed **PMAS2** is the least favored structure over the entire temperature range. These ΔG calculations clearly establish that at very low temperatures (around 10 K) the observed structures of H$_2$O (**PWS3**), NH$_3$ (**PAS1**), and to some extent MeOH (**PMS2**) complexes are thermodynamically the most favored structures. However, it must be noted that in the case of MeOH complex, the difference in the energies of the three is about 0.4 kJ mol^{-1}, which is about the accuracy of the level of calculations reported here. The exclusive observation of **PMS2** structure clearly indicates that there might be effects that clearly cannot be distinguished by the present set of stabilization energy and thermochemical calculations. The exclusive formation of the **PMS2** structure can perhaps be explained as follows. If we consider that a single collision in the molecular beam between PHA and MeOH moieties leads to the formation of the binary complex, then the cross-section for such a collision will be the largest with the π electron density of the benzene ring relative to the two other binding sites. This higher cross-section offered by the π electron density of the benzene ring can be interpreted as an entropic advantage of this
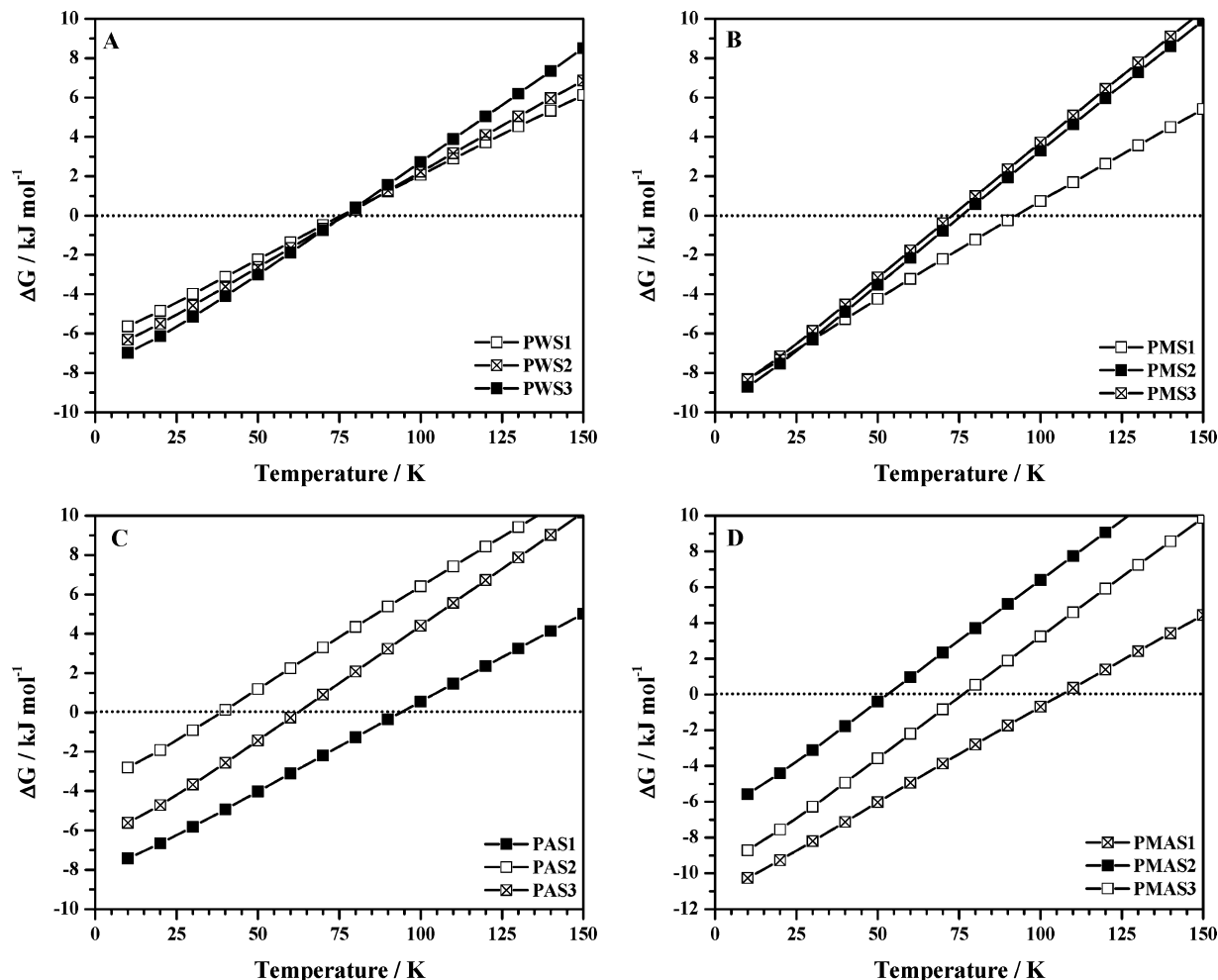
Figure 3. Plot of variation of ΔG vs T for the formation of various complexes of PHA with (A) H_2O, (B) MeOH, (C) NH_3, and (D) $MeNH_2$ (see text for details). In each case the solid squares (■) represent the experimentally observed structure.

site over the other two binding sites. However, it should be noted at this point that the entropy contribution in the thermochemical calculation of ΔG is purely based on the partition function of a particular structure based on rigid rotor−harmonic oscillator−ideal gas approximation (see Methodology), which is different from the system entropy based on the interaction cross-section. This entropic advantage in combination with lower ΔG (marginally lower by 0.4 kJ mol^{-1}) manifests in the formation of the **PMS2** structure.

Similar arguments can be used in the case of the $MeNH_2$ complex, wherein the exclusive formation of the **PMAS2** structure can be attributed to the larger cross-section of interaction offered by the π electron density of the benzene ring. However, unlike the MeOH complex (**PMS2**), the $MeNH_2$ complex (**PMAS2**) is thermodynamically unfavorable over the other two complexes, especially **PMAS1**, which at 10 K is more stable by 4.7 kJ mol^{-1}. This implies that the population of **PMAS2** should be negligibly low. Nevertheless, the **PMAS2** complex is exclusively formed. Clearly the thermodynamic factors cannot explain such an observation. An alternative explanation based on the kinetics can be as follows: The **PMAS2** structure is a stable minimum and forms during the initial phase of supersonic expansion. However, if the barrier for its interconversion to the most stable minimum **PMAS1** is sufficiently high enough to be surmounted at the temperatures prevailing in the supersonic jet,[20] then the PHA−$MeNH_2$ complex is trapped in the higher energy minimum, which in the present case is **PMAS2**. Therefore, the observation of higher energy

PMAS2 in the present experimental conditions can therefore be attributed to the kinetic trapping.[21] It must be emphasized here that in the absence of any experimental evidence, this explanation can only at best be tentative.

The ability of formation of H_2O and NH_3 to form the thermodynamically most stable structures can be interpreted on the basis of dominance of the electrostatic contribution to the total energy. On the other hand, for the MeOH and $MeNH_2$ complexes, the higher polarizability of the O−H and N−H groups favor interaction with the π electron density of the benzene ring, wherein the dispersion forces dominate. This, accompanied by the ability of π electron density of the benzene ring to offer a higher cross-section of interaction, leads to the formation of MeOH and $MeNH_2$ complexes. In addition, kinetic trapping plays a pivotal role in the formation of the observed PHA−$MeNH_2$ complex. Thus, in multifunctional molecules the exact hydrogen bonding pattern will be a result of subtle competition between various possibilities, which depends on the fine interplay between the electrostatic and dispersion forces.

Conclusions

The hydrogen-bonded complexes of PHA with H_2O, MeOH, NH_3, and $MeNH_2$ form a variety of intermolecular structures. The H_2O complex is characterized by the presence of O−H···π and C−H···O hydrogen bonds, while the O−H group of MeOH interacts with the π electron density of the benzene ring. NH_3 forms a linear C−H···N σ hydrogen-bonded complex. On the

Hydrogen-Bonded Complexes of Phenylacetylene

J. Phys. Chem. A, Vol. 113, No. 24, 2009 **6625**

other hand, the MeNH$_2$ complex is stabilized by the presence of N−H···π hydrogen bonding accompanied by a peripheral interaction of methyl C−H group with the acetylenic C≡C bond. The stabilization energies calculated at CCSD(T)/aug-cc-pVDZ level along with the calculated values of ΔG for the formation of various complexes reveal that the observed complexes of H$_2$O and NH$_3$ are the most stable minima. The MeOH complex is also the most stable minimum; however, its relative stability is only marginally higher than the other two minima. The observed MeNH$_2$ complex is the highest energy structure both in terms of stabilization and free energies and definitely is a kinetically trapped structure. The DFT-SAPT calculations indicate that electrostatics play a dominant role in stabilizing the observed H$_2$O and NH$_3$ complexes, while dispersion is the major contribution for the MeOH and MeNH$_2$ complexes. The subtle balance between the electrostatic and dispersion forces along with factors such as surface area of interaction and kinetic trapping lead to the observed methyl group-induced hydrogen bond switching in the phenylacetylene complexes.

References and Notes

(1) (a) Etter, M. C. *Acc. Chem. Res.* **1990**, *23*, 120. (b) Etter, M. C. *J. Phys. Chem.* **1991**, *95*, 4601.

(2) Legon, A. C.; Millen, D. J. *Chem. Soc. Rev.* **1987**, *16*, 467.

(3) Singh, P. C.; Bandyopadhyay, B.; Patwari, G. N. *J. Phys. Chem. A* **2008**, *112*, 3360.

(4) Singh, P. C.; Patwari, G. N. *J. Phys. Chem. A* **2008**, *112*, 5121.

(5) Singh, P. C.; Patwari, G. N. *J. Phys. Chem. A* **2008**, *112*, 4426.

(6) (a) Engdahl, A.; Nelander, B. *J. Phys. Chem.* **1985**, *89*, 2860. (b) Wanna, J.; Menapace, J. A.; Bernstein, E. R. *J. Chem. Phys.* **1986**, *85*, 1795. (c) Suzuki, S.; Green, P. G.; Bumgarner, R. E.; Dasgupta, S.; Goddard, W. A., III; Blake, G. A. *Science* **1992**, *257*, 942. (d) Pribble, R. N.; Garrett, A. W.; Haber, K.; Zwier, T. S. *J. Chem. Phys.* **1995**, *103*, 531. (e) Gutowsky, H. S.; Emilsson, T.; Arunan, E. *J. Chem. Phys.* **1993**, *99*, 4883.

(7) (a) Engdahl, A.; Nelander, B. *Chem. Phys. Lett.* **1983**, *100*, 129. (b) Peterson, K. I.; Klemperer, W. *J. Chem. Phys.* **1984**, *81*, 3842.

(8) Fraser, G. T.; Leopold, K. R.; Klemperer, W. *J. Chem. Phys.* **1984**, *80*, 1423.

(9) (a) Jeziorski, B.; Moszynski, R.; Szalewicz, K. *Chem. Rev.* **1994**, *94*, 1887. (b) Hesselman, A.; Jansesn, G.; Schutz, M. *J. Chem. Phys.* **2005**, *122*, 14103.

(10) Frisch, M. J.; Trucks, G. W.; Schlegel, H. B.; Scuseria, G. E.; Robb, M. A.; Cheeseman, J. R.; Montgomery, J. A., Jr.; Vreven, T.; Kudin, K. N.; Burant, J. C.; Millam, J. M.; Iyengar, S. S.; Tomasi, J.; Barone, V.; Mennucci, B.; Cossi, M.; Scalmani, G.; Rega, N.; Petersson, G. A.; Nakatsuji, H.; Hada, M.; Ehara, M.; Toyota, K.; Fukuda, R.; Hasegawa, J.; Ishida, M.; Nakajima, T.; Honda, Y.; Kitao, O.; Nakai, H.; Klene, M.; Li, X.; Knox, J. E.; Hratchian, H. P.; Cross, J. B.; Bakken, V.; Adamo, C.; Jaramillo, J.; Gomperts, R.; Stratmann, R. E.; Yazyev, O.; Austin, A. J.; Cammi, R.; Pomelli, C.; Ochterski, J. W.; Ayala, P. Y.; Morokuma, K.; Voth, G. A.; Salvador, P.; Dannenberg, J. J.; Zakrzewski, V. G.; Dapprich, S.; Daniels, A. D.; Strain, M. C.; Farkas, O.; Malick, D. K.; Rabuck, A. D.; Raghavachari, K.; Foresman, J. B.; Ortiz, J. V.; Cui, Q.; Baboul, A. G.; Clifford, S.; Cioslowski, J.; Stefanov, B. B.; Liu, G.; Liashenko, A.; Piskorz, P.; Komaromi, I.; Martin, R. L.; Fox, D. J.; Keith, T.; Al-Laham, M. A.; Peng, C. Y.; Nanayakkara, A.; Challacombe, M.; Gill, P. M. W.; Johnson, B.; Chen, W.; Wong, M. W.; Gonzalez, C.; Pople, J. A. Gaussian 03, Revision A.1; Gaussian, Inc., Wallingford, CT, 2003.

(11) Amos, R. D.; Bernhardsson, A.; Berning, A.; Celani, P.; Cooper, D. L.; Deegan, M. J. O.; Dobbyn, A. J.; Eckert, F.; Hampel, C.; Hetzer, G.; Knowles, P. J.; Korona, T.; Lindh, R.; Lloyd, A. W.; McNicholas, S. J.; Manby, F. R.; Meyer, W.; Mura, M. E.; Nicklass, A.; Palmieri, P.; Pitzer, R.; Rauhut, G.; Schü tz, M.; Schumann, U.; Stoll, H.; Stone, A. J.; Tarroni, R.; Thorsteinsson, T.; Werner, H.-J. MOLPRO, a package of ab initio programs, version 2006.1.

(12) Stearns, J. A.; Zwier, T. S. *J. Phys. Chem. A* **2003**, *107*, 10717.

(13) Singh, P. C.; Patwari, G. N. *Curr. Sci.* **2008**, *95*, 469.

(14) (a) Siglow, K.; Neusser, H. J. *Chem. Phys. Lett.* **2001**, *343*, 475. (b) Dreizler, H.; Hartke, B.; Rudolph, H. D. *J. Mol. Struct.* **2006**, *825*, 1.

(15) Lakshmi, B.; Samuelson, A. G.; Jose, K. V. J.; Gadre, S. R.; Arunan, E. *New J. Chem.* **2005**, *29*, 371.

(16) Rodham, D. A.; Suzuki, S.; Suenram, R. D.; Lovas, F. J.; Dasgupta, S.; Goddard, W. A., III; Blake, G. A. *Nature* **1993**, *362*, 735.

(17) The other spectroscopic inputs include the shift in the electronic transitions for the complexes relative to the bare PHA and the IR spectra in the O−H stretching region for the H$_2$O and MeOH complexes. See refs 3−5 for details.

(18) Dabkowska, I.; Jurecka, P.; Hobza, P. *J. Chem. Phys.* **2005**, *122*, 204322.

(19) (a) Janowski, T.; Pulay, P. *Chem. Phys. Lett.* **2007**, *447*, 27. (b) Jurečka, P.; Šponer, J.; Černý, J.; Hobza, P. *Phys. Chem. Chem. Phys.* **2006**, *8*, 1985.

(20) It is difficult to precisely comment on the temperature during the expansion process, but it should lie between the nozzle temperature (298 K) and the terminal temperature (∼3.5 K for phenylacetylene).

(21) (a) Douberly, G. E.; Ricks, A. M.; Schleyer, P. v. R.; Duncan, M. A. *J. Chem. Phys.* **2008**, *128*, 021102. (b) Maity, S.; Patwari, G. N. *J. Phys. Chem. A* **2009**, *113*, 9702.